Int J Thermophys (2008) 29:1014–1025
DOI 10.1007/s10765-008-0403-3

Middle Temperature Scale for Infrared Radiation Thermometer Calibrated Against Multiple Fixed Points

Y. Shimizu · J. Ishii

Published online: 8 May 2008

Abstract The NMIJ has established a temperature scale for infrared radiation thermometry from 100 to 420°C consisting of three fixed-point blackbodies at the In, Sn, and Zn points and an InSb detector thermometer at a wavelength of 4.7 µm. The blackbody cavities have large openings of 15 mm diameter. The expanded uncertainties ($k = 2$) of the In, Sn, and Zn fixed-point radiance temperatures are estimated to be 0.03, 0.03, and 0.05 K, respectively. The expanded uncertainties ($k = 2$) for the calibration of the infrared radiation thermometer are estimated to be 0.04 K at 157°C (In point), 0.04 K at 232°C (Sn point), and 0.07 K at 420°C (Zn point).

Keywords Infrared radiation thermometer · InSb detector · Middle temperature · Multiple fixed points · Temperature scale

1 Introduction

The National Metrology Institute of Japan (NMIJ) has previously described its calibration facilities for radiation thermometry in the high-temperature range from 400 to 2500°C [1] and the low-temperature range from −30 to 160°C [2]. The former consists of a copper-point blackbody and a near-infrared radiation thermometer with a Si photodiode and the latter consists of a variable-temperature blackbody with a reference platinum resistance thermometer (PRT) sensor traceable to the International Temperature Scale of 1990 (ITS-90) and an infrared radiation thermometer with a cryogenically cooled InSb photodiode. Recently, infrared radiation thermometry in the so-called 'middle temperature range' has become widely used in the fields of industrial process control, thermal management, thermography, remote sensing, and

Y. Shimizu (✉) · J. Ishii
National Metrology Institute of Japan (NMIJ), AIST, Tsukuba, Japan
e-mail: shimizu-yukiko@aist.go.jp

non-destructive inspection. The authors have developed a calibration facility with an infrared radiation thermometer specially designed for the temperature range from 100 to 420°C to meet a rapidly increasing demand by industry for the calibration of infrared instruments.

Several preceding studies have been reported for this temperature range. The TRIRAT (traceability in infrared radiation thermometry) project was started in 1996 [3]. An inter-comparison among the temperature scales of 14 metrological laboratories was successfully carried out with an InGaAs detector-based radiation thermometer in the range from 150 to 962°C. The Istituto di Metrologia "G. Colonnetti" (IMGC, now INRiM) constructed a near-infrared thermometer with an InGaAs photodiode cooled to −10°C and the fixed-point blackbodies of In, Sn, Zn, Al, and Ag for the temperature range from 150 to 1000°C [4]. The National Physical Laboratory (NPL) performed measurements using a radiation thermometer with an InGaAs detector and fixed-point blackbody sources at the Sn, Pb, Zn, Al, and Ag points for the temperature range from 232°C (Sn) to 962°C (Ag) [5]. The PTB developed an infrared radiation thermometer with an InGaAs detector as a transfer standard in the temperature range from 150 to 960°C. A sodium heat-pipe blackbody, a cesium heat-pipe blackbody, and a water heat pipe were used as reference calibration sources [6–8].

These preceding reports mostly employed InGaAs detectors working at 1.6 μm. In the range below 200°C, the InGaAs thermometer has relatively low sensitivity [9,10]. The present article describes the establishment of a temperature scale with a 4.7 μm InSb infrared thermometer calibrated at the In (157°C), Sn (232°C), and Zn (420°C) fixed points in the middle temperature range. An InSb detector and fixed-point blackbodies are successfully employed in a calibration facility for the first time, to our knowledge.

2 Calibration Facilities

2.1 Blackbody Cavity with a Large Opening

The In, Sn, and Zn fixed-point blackbodies are used to cover the middle temperature range from 100 to 420°C. The design and a performance of the Zn-point blackbody was described in [11]. The same type of cavities are used for In and Sn. Each blackbody has a cylindrical cavity with a large opening of 15 mm diameter, so that the size-of-source effect (SSE) becomes small for the calibration of the infrared thermometer. The cavity has a depth of 105 mm and is terminated in a cone with an apex angle of 120°. The insides of the cavities are grooved with 1 mm pitch to increase the emissivity. As will be discussed later, the effective emissivity is estimated to be 0.9991 ± 0.0001. The purities of the metals filling the crucible were 99.9999% in all cases. The quality of the plateau critically depends on the temperature distribution in the cavity. The crucible is placed within a three-zone electrically heated furnace. The temperatures of the heaters in the front and rear zones are set several degrees higher than that of the main zone to reduce the temperature gradient along the length of the cavity.

The temperature variation along the outer wall of the crucible was within 200 mK at the Zn point. The measurements were carried out by moving a Type K thermocouple

along the grooved guide in the outer wall of the crucible, and this measurement was repeated three times with three identical thermocouples; thus, nine series of measurements were performed. The thermocouples were annealed for 5 h at 800°C, and then 5 h at 450°C, before every measurement to minimize inhomogeneity. The length of the uniform temperature region of this annealing furnace is 200 mm, which is enough longer than the length of the crucible (135 mm) to ensure homogeneity. Each measurement was performed within 20 min to reduce the influence of inhomogeneity. The temperature distribution obtained by the nine measurements shows good reproducibility, and the maximum temperature difference of each measurement is within 200 mK. Considering these results, the temperature distribution of the outer crucible wall is conservatively estimated to be within 500 mK.

The freezing plateaux of In, Sn, and Zn observed by the InSb thermometer are shown in Fig. 1. They last 70, 40, and 70 min, respectively, at the optimum conditions where the shapes and repeatabilities of the plateaux are good. The uncertainties of the radiance temperatures of the fixed-point blackbodies are discussed in Sect. 4.

2.2 InSb Infrared Radiation Thermometer

The design and construction of the infrared radiation thermometer were described in [11]. A cross-sectional view of the infrared radiation thermometer constructed for the middle temperature range is shown in Fig. 2. The optical components, except the objective lens, are assembled in a cryogenic vacuum chamber, and the thermometer is operated in the dc mode without a mechanical chopper. The thermometer is designed to work at a fixed target distance of 1000 mm from the objective lens of 50 mm effective diameter. Two sighting lasers with beams crossing each other at the focus position are attached to the front face of the objective lens to simplify targeting.

The inside of the cold radiation shield is grooved to prevent inter-reflection of scattered light. The outer surface of the cold radiation shield is polished to reduce thermal exchange with ambient radiation. The volume of the cold radiation shield is twice that of the previous one [11], so that it is more difficult for stray light to reach the sensor after multiple reflections.

The dielectric interference filter has a center wavelength of 4.7 µm and a spectral bandwidth (full width at half maximum (FWHM)) of 0.34 µm at 77 K and is placed inside the cold radiation shield. Within this bandwidth, there are no absorption lines from atmospheric molecules such as CO_2 and H_2O.

3 Calibration Equation

The present calibration scheme incorporates a modified Sakuma-Hattori interpolation equation [12] based on Planck's law;

$$S(T) = \frac{C}{\exp\{c_2/(AT + B)\} - 1} + D, \tag{1}$$

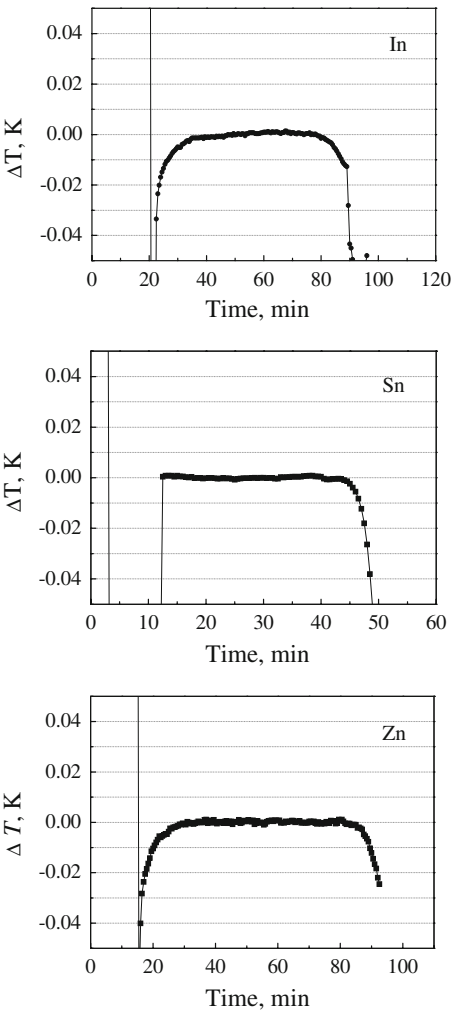

Fig. 1 Observed plateaux of the In, Sn, and Zn fixed points as measured by the InSb thermometer

where $S(T)$ is the output of the thermometer and A, B, and C are parameters to be determined from the calibration at the three fixed points. In the present case of infrared detection, ambient radiation cannot be neglected. This effect is introduced in Eq. 1 by an offset term, D. The value of D can be experimentally determined by observing a cavity made from ice, which is considered to be a practically zero radiation target relative to the measuring range. The ice cavity is 50 mm in diameter and 126 mm in depth and terminates in a cone with an apex angle of 120°.

4 Uncertainties of the Temperature Scale

The temperature scale in the range from 100 to 420°C has been established with an infrared thermometer calibrated using three fixed-point blackbodies. The interpolated

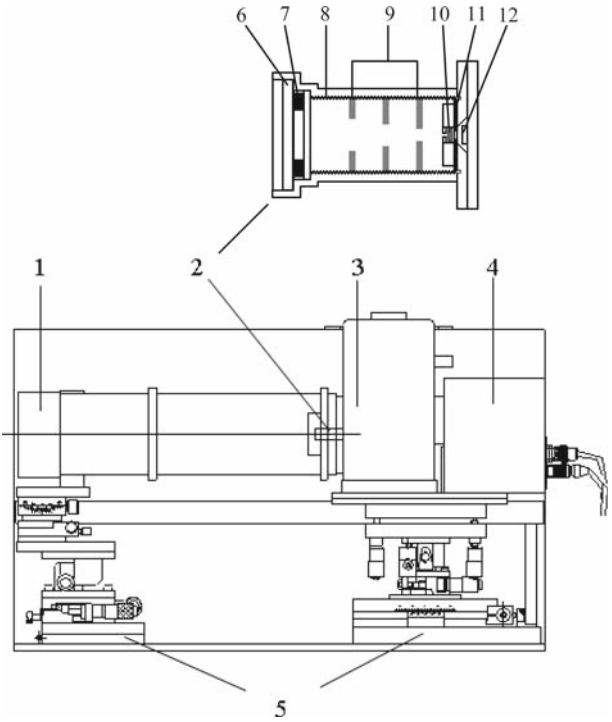

Fig. 2 Cross-sectional views of the InSb radiation thermometer; 1: achromatic doublet lens and holder, 2: cold radiation shield, 3: liquid nitrogen Dewar, 4: amplifier, 5: alignment stage, 6: interference filter, 7: aperture stop, 8: grooved spacer, 9: baffles, 10: field lens, 11: field stop, 12: detector

and extrapolated temperatures are determined from the thermometer output by using Eq. 1. The parameters A, B, C, and D are determined from the thermometer outputs at the three metal fixed points and the ice point. The uncertainty budget of the realized temperature scale is summarized in Table 1 and elaborated below.

When the temperature of an unknown radiation source is determined, other uncertainties (in-use uncertainty components) due to the measured thermometer signal, the nature of the radiation source, ambient temperature, etc. should be taken into account. However, this is omitted from the uncertainties of our temperature scale and is not discussed further here.

Numerical estimates of the individual component uncertainties are given in the following sections.

4.1 Uncertainties in the Calibration and Determination of the Interpolation Function

This item of the uncertainty budget, which describes the uncertainties of the calibration and the determination of the interpolation function, is characteristic of the calibration facility and consists of the following components.

Table 1 Uncertainty components in temperature scale with fixed-point blackbodies for the radiation thermometers

Uncertainty components	Temperature (°C)									
	100	150	157(In)	200	232(Sn)	250	300	350	400	420(Zn)
	Uncertainty (mK)									
(4.1) Uncertainties in the calibration and determination of the interpolation function										
(4.1.1) Quality of match of the interpolation equation (Interpolation error)	1	1	1	1	1	1	1	1	1	1
(4.1.2) Uncertainties in determining the coefficients A, B, C, and D										
(4.1.2.1) Uncertainties of the fixed-point temperatures										
(4.1.2.1.1) Identification of the plateau			3		2					2
(4.1.2.1.2) Repeatability of the plateau			12		3					3
(4.1.2.1.3) Re-installation of the cavity crucible			1		1					1
(4.1.2.1.4) Effective emissivity of the blackbody			5		7					13
(4.1.2.1.5) Impurities in the fixed-point metal			2		1					1
(4.1.2.1.6) Temperature distribution within the blackbody furnace			9		12					23
Combined uncertainty ($k = 1$) of (4.1.2.1)			16		14					27
(4.1.2.2) Uncertainty of the thermometer signal										
(4.1.2.2.1) Effect of ambient temperature			11		13					22
(4.1.2.2.2) Alignment of the thermometer			3		4					8
(4.1.2.2.3) Detector noise and non-linearity			1		1					1
Combined uncertainty ($k = 1$) of (4.1.2.2)			11		14					23
(4.1.2.3) Uncertainty in determining the offset term D			8		4					1
Combined uncertainty ($k = 1$) of the item(4.1.2)			21		20					35
(4.2) Uncertainties propagated through the interpolation equation	51	24		15		26	26	26	31	
Combined uncertainty ($k = 1$)	51	24	21	15	20	26	26	26	31	35
Expanded uncertainty ($k = 2$)	102	48	43	30	41	52	52	52	62	71

A, B, C, and D are parameters in the interpolation equation. The item numbers in the table correspond to the section number in the text

4.1.1 Interpolation Error

Saunders and White [13] discussed the interpolation error introduced by using Eq. 1 for various spectral response functions. When the calibration temperatures of T_1, T_2, and T_3 are equally spaced, the peak value of the error in temperature is simply expressed by

$$|\Delta T|_{\text{peak}} = \frac{E{\lambda_0}^2{T_{\text{range}}}^3}{a}, \tag{2}$$

where λ_0 is the mean wavelength of the spectral responsivity and T_{range} is the temperature calibration range. For well-defined spectral responsivities such as Gaussian and rectangular functions, the coefficient E is a function of $x = \lambda_0 T_{\text{m}}$ (T_{m} is the mean temperature of the interpolation range) and $r = \sigma/\lambda_0$ (σ is the standard deviation of the spectral response). Saunders and White [13] numerically calculated this coefficient, and the results were graphically represented as functions of x and r. A numerical constant, a, depends on the shape of the responsivity and takes a value of $12\sqrt{3}$ for a Gaussian responsivity. In the present case, $\lambda_0 = 4.7\,\mu\text{m}$, $T_{\text{range}} = 320\,\text{K}$, $T_{\text{m}} = 562\,\text{K}$, and $\sigma = 0.34\,\mu\text{m}/\sqrt{2\ln 2} = 0.288\,\mu\text{m}$ (the FWHM of the responsivity is 0.34 µm). For the Gaussian responsivity, the value of E at $\lambda_0 T_{\text{m}} = 0.0026$ and $\sigma/\lambda_0 = 0.0031$ obtained from the graph for Gaussian responsivity (Fig. 3 of [13]) is $E = 30\,\text{m}^{-2}\cdot\text{K}^{-2}$ and then ΔT is calculated to be 0.6 mK. Saunders and White pointed out that for unequally spaced fixed-point temperatures, ΔT is somewhat larger than Eq. 2.

The actual spectral function of the filter may have a longer tail than that of a Gaussian. The effect of a tail on ΔT is calculated by using a Gaussian responsivity (center: 4.7 µm and FWHM: 0.34 µm) with a positive constant bias of 10^{-3} over a wavelength range five times the FWHM. The uncertainty ΔT estimated for the Gaussian responsivity (0.6 mK) increases due to the effect of the tail by 2.5% at 100°C, 0.8% at 200°C, and 0.3% at 400°C. Therefore, the interpolation error is not larger than 1 mK throughout the temperature range.

4.1.2 Uncertainties in Determining the Coefficients A, B, C, and D

Uncertainties in determining the coefficients A, B, C, and D comprise uncertainties of the fixed-point temperatures, uncertainties of the thermometer signal, and uncertainty in determining the offset term D.

4.1.2.1 Uncertainties of the Fixed-Point Temperatures The uncertainty of the fixed-point temperatures includes components for the identification of the plateau, the repeatability of the plateau, re-installation of the crucible, the effective emissivity of the blackbody, impurities in the fixed-point metal, and the temperature distribution within the furnace.

4.1.2.1.1 Identification of the Plateau The fixed-point temperature is determined from the average of the points from 25 to 75% of the plateau duration and the uncertainty is the plateau width, defined as the standard deviation of the statistically scattered observed points in the above range. The freezing plateaux obtained at the three fixed points are shown in Fig. 1. The uncertainties are 3 mK for In, 2 mK for Sn, and 2 mK

for Zn. The long duration and the flatness of the observed plateaux can determine the fixed-point temperatures precisely.

4.1.2.1.2 Repeatability of the Plateau The repeatability of the freezing plateaux was experimentally checked with ten plateau realizations within a week using the InSb infrared radiation thermometer (described herein) and the InGaAs thermometer [6]. The room temperature was kept within 1°C throughout the experiment. The uncertainties attributed to the repeatability were 13 mK for In, 4 mK for Sn, and 8 mK for Zn ($k = 1$) with the InSb thermometer; 12 mK for In, 3 mK for Sn, and 3 mK for Zn ($k = 1$) were obtained with the InGaAs thermometer. These uncertainties should be considered to represent long-term instabilities arising from various sources. They include uncertainties due to fluctuation and drift of the thermometers and to instabilities of the fixed-point temperatures. It is difficult to separate the uncertainty into contributions from the individual sources. Since the InGaAs thermometer shows better stability and is less sensitive to radiation from ambient temperature, the above results with the InGaAs thermometer are taken as the upper limits of uncertainty for the fixed-point radiation temperatures (Sect. 4.1.2.1.2), and they are listed in Table 1 as part of the uncertainty budget. As will be discussed later in Sect. 4.1.2.2.1, changes in ambient temperature have less influence on the observed temperatures of the fixed points than the values of the uncertainties shown here. The uncertainty at the In point is fairly large compared to the values at the Sn and Zn points. This may be due to the fact that the thermometers show a smaller signal-to-noise ratio at the lower temperature.

4.1.2.1.3 Re-installation of the Cavity Crucible The temperatures of the blackbodies at the three fixed points measured by the InSb thermometer were reproduced within 1 mK when the fixed-point crucible assemblies were exchanged.

4.1.2.1.4 Effective Emissivity of the Blackbody The effective emissivity of the cavity depends on its shape, the intrinsic emissivity of the inner surface material, and the machining imperfections. The shape-dependent effective emissivity of the cavity is estimated from a Monte Carlo calculation [14] that assumes an isothermal cavity and a perfectly diffuse reflection at the cavity surface. For this calculation, the intrinsic emissivity of the actual surface material of the cavity is required. The intrinsic emissivity of the graphite was measured with the FTIR method [15]. It is noted that the emissivity depends on the surface condition; a value of 0.85 was found for the diffuse surface and 0.80 for the well-polished surface at a wavelength near 5 μm (the working wavelength of the thermometer). The cavity emissivities are calculated to be $\varepsilon_1' = 0.9992$ for the diffuse surface intrinsic emissivity of $\varepsilon_1 = 0.85$ and $\varepsilon_2' = 0.9989$ for the polished surface intrinsic emissivity of $\varepsilon_2 = 0.80$. It is assumed that the emissivity of the present cavity falls between these two values, and the difference is considered the uncertainty in estimating the emissivity. The resulting uncertainties of the blackbody radiation temperatures attributed to the uncertainty in the emissivity were evaluated to be 5 mK for In, 7 mK for Sn, and 13 mK for Zn. For the present cavities, the uncertainty due to machining imperfections [16] is estimated to be 0.3 mK, and therefore negligible.

4.1.2.1.5 Impurities in the Fixed-Point Metal Impurities in the metal filling the crucible generally depress the plateau temperature and also reduce the quality of the plateau. The purities of the metals filling the crucibles are 99.9999% in all cases (In, Sn, and Zn). The effect of impurities is estimated on the basis of the temperature depression due to the nominal impurity content of the metal samples. The molar

cryoscopic constants for In, Sn, and Zn are calculated from their melting enthalpies and melting temperatures to be $25\,\mathrm{K}\cdot\mathrm{kg}\cdot\mathrm{mol}^{-1}$ for In, $36\,\mathrm{K}\cdot\mathrm{kg}\cdot\mathrm{mol}^{-1}$ for Sn, and $40\,\mathrm{K}\cdot\mathrm{kg}\cdot\mathrm{mol}^{-1}$ for Zn [17]. The most probable impurity is Si in the cases of In and Zn and Au in the case of Sn. The molar concentrations of Si and Au for the metals with 6N purity are $3.6\times10^{-5}\,\mathrm{mol}\cdot\mathrm{kg}^{-1}$ and $5.1\times10^{-6}\,\mathrm{mol}\cdot\mathrm{kg}^{-1}$, respectively. The depressions of freezing-point temperatures are calculated to be 1.5 mK for In, 1.3 mK for Sn, and 1.4 mK for Zn. These values are considered to be the uncertainties of the fixed-point temperatures caused by impurities.

4.1.2.1.6 Temperature Distribution within the Blackbody Furnace The major contribution to the uncertainty in the repeatability of radiance temperature may be the temperature distribution throughout the cavity. Since it is difficult to measure the temperature distribution in the cavity, we measure a change in the blackbody temperature when a temperature gradient is imposed on the crucible. When a temperature difference of 500 mK exists between the front and back of the crucible, the plateau temperature changes by 9 mK for In, 12 mK for Sn, and 23 mK for Zn. These values are taken as the upper limits of uncertainties in blackbody temperature due to the temperature distribution in the cavity, as shown in Table 1. This is because the furnace currents are controlled so that the temperature difference along the crucible does not exceed 500 mK. Actually, the temperature difference measured under typical conditions was 200 mK, as stated in Sect. 2.1.

4.1.2.2 Uncertainty of the Thermometer Signal The uncertainty of the thermometer signal, $\Delta S(T)/S(T)$, is transferred to the uncertainty of the blackbody temperature according to

$$\Delta T = \frac{\lambda T^2}{c_2}\frac{\Delta S}{S}\left(1-\exp\left[-\frac{c_2}{\lambda T}\right]\right) \tag{3}$$

which is derived by differentiation of Eq. 1. That is to say, the effective temperatures of the fixed-point blackbodies are assumed to change by ΔT because of the uncertainty of the detector output. The change in the effective temperatures of blackbodies at the fixed points propagates to other temperatures, as described later in Sect. 4.2. The uncertainty of the thermometer signal combines the effect of ambient temperature, the alignment of the thermometer, and detector noise and non-linearity.

4.1.2.2.1 Effect of Ambient Temperature on the Thermometer Signal The instability of the thermometer output caused by ambient temperature change is measured by changing the room temperature from 22 to 24°C while the thermometer is measuring the fixed-point blackbodies of In, Sn, and Zn. A small platinum resistance thermometer is placed near the objective lens to monitor the effective ambient temperature. Ten series of experiments were repeated over several days. The uncertainty was evaluated from all scattered data points, assuming a rectangular distribution. The uncertainties in the InSb thermometer output for room-temperature fluctuation within 2°C corresponds to temperature uncertainties of 12 mK for the In point, 13 mK for the Sn point, and 22 mK for the Zn point. These include the effects on both the thermometer and the fixed-point temperatures. To separate the effect due to the variations of the apparent blackbody temperatures, experiments were also carried out with the InGaAs thermometer, which was much more stable with respect to a change of room temperature.

The plateau was observed at room temperatures of 22°C, 23°C, and 24°C for each fixed-point blackbody during a day. The analysis of the changes in the plateau temperatures leads to estimates of 4 mK for the In point, 1 mK for the Sn point, and 1 mK for the Zn point as the approximate uncertainties of the fixed-point temperatures caused by a room temperature change of 2°C, and they can be separated from the changes observed with the InSb thermometer to obtain the differences listed as an item (Sect. 4.1.2.2.1) of Table 1.

4.1.2.2.2 Alignment of the Thermometer The thermometer was removed and re-mounted, and then the calibration cycle was repeated on the same day. The resettability of the alignment gives an uncertainty of less than 5 mK for all three fixed points.

4.1.2.2.3 Detector Noise and Non-linearity The peak-to-peak noise of the detector for measurements of fixed-point blackbodies is transferred to the uncertainty in blackbody temperature by using Eq. 3. This is less than 1 mK throughout the observed temperature range. It is difficult to measure the non-linearity effect in the infrared region; therefore, the effect is evaluated as follows. Regarding the non-linearity of the InSb detector, it is reported that the detector should be linear in the modest range of $L(800°C)/L(157°C) = 176$, while for the wider range of $L(960°C)/L(20°C) = 15500$, a nonlinearity of 1×10^{-3} (normal thermometer) or 1×10^{-4} (best thermometer) is expected [16,18]. Here, L is the Planck radiance. In our case, the range $L(420°C)/L(100°C) = 12$ falls well within the modest range. Even if a non-linearity of 1×10^{-3}(normal thermometer) is assumed, it is expected to be $1 \times 10^{-3} \times (12/15500) = 0.8 \times 10^{-6}$ for the present range; the uncertainty in temperature becomes about 0.1 mK at 420°C (Zn point), which is fairly small compared to the detector noise and it is therefore omitted from the uncertainty budget.

4.1.2.3 Uncertainty in Determining the Offset Term D The uncertainties of the apparent blackbody temperatures caused by the standard deviation of repeatedly observed D values are calculated using Eq. 3 at the three fixed-point temperatures. The values are 8 mK for the In point, 4 mK for the Sn point, and 1 mK for the Zn point. They are listed as a component (Sect. 4.1.2.3) of Table 1. These uncertainties propagate to the temperatures determined with Eq. 1.

4.2 Uncertainties Propagated Through the Interpolation Equation

The uncertainties caused by the various sources stated above are expressed in temperature and tabulated in Table 1. In the case of In, for example, the combined uncertainty of the blackbody is 16 mK for the item presented in Sect. 4.1.2.1 and the combined uncertainty in the thermometer signal for the item presented in Sect. 4.1.2.2 is 11 mK. The resulting standard uncertainty of the root-sum-square, 19 mK, causes uncertainties in the parameters of Eq. 1, and then the temperature interpolated by Eq. 1 has the propagated uncertainty.

The propagated uncertainty is calculated in the following way. For each of the three fixed-point temperatures, we calculate how much the interpolated temperature changes when any one of these base temperatures is shifted by its uncertainty. First, the temperature T is calculated using primary values of the parameters A, B, and C determined

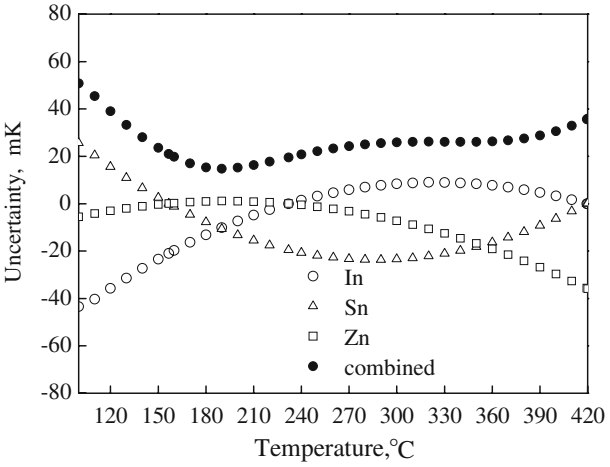

Fig. 3 Propagation of uncertainties for the fixed-point temperatures, the uncertainties in the thermometer signal, and the uncertainty in determining the offset term D through the interpolation equation. Open circles are for In, triangles for Sn, squares for Zn, and black circles for the combined uncertainty

from the defined blackbody temperatures. Then, the parameters are re-determined to be A', B', and C', from the In temperature shifted by 20 mK. The temperature T' is calculated using A', B', and C'. The temperature difference $|T - T'| = \Delta T$ gives the propagated uncertainty for the In point. The result is shown in Fig. 3 with open circles. The same procedures are carried out for temperature shifts of 20 mK at the Sn point and 36 mK at the Zn point. The results of the calculation are shown in Fig. 3 as functions of temperature for 50°C steps, as indicated by the open triangles and open squares. The combined uncertainty due to the three calibration points is shown in Fig. 3 as filled circles. The values for temperatures within the temperature range are listed under the item presented in Sect. 4.2 of Table 1 as the propagated uncertainty due to the calibration of the InSb thermometer.

5 Conclusion

We have shown that an InSb infrared radiation thermometer calibrated at three fixed-point temperatures, In, Sn, and Zn, can realize an accurate temperature scale between 100°C and 420°C. The expanded uncertainties ($k = 2$) of the radiance temperature of the blackbodies are estimated to be 0.03, 0.03, and 0.05 K, respectively. The uncertainty budget for the present calibration facility with the infrared radiation thermometer and the In, Sn, and Zn fixed-point blackbodies was evaluated as shown in Table 1. The expanded uncertainties ($k = 2$) of the calibration with the InSb radiation thermometer are estimated to be 0.04 K at 157°C (In point), 0.04 K at 232°C (Sn point), and 0.07 K at 420°C (Zn point). When the unknown temperature of a radiation source is determined with this calibration facility, the nature of the unknown radiation source should be added to the above uncertainties. In conclusion, the estimated expanded uncertainty of the present calibration facility is less than 0.1 K in the temperature range from 100

to 420°C and the performance is good enough to calibrate the radiation thermometers and blackbodies used by industry.

Acknowledgment The authors would like to thank Ms. K. Minahiro of NMIJ for her contribution to the experimental measurements.

References

1. F. Sakuma, L. Ma, Calibration facilities for high temperature radiation thermometers at NMIJ, in *Proceedings of SICE-ICASE International Joint Conference 2006*, Busan, Korea (2006), pp. 3336–3341
2. J. Ishii, A. Ono, in *Temperature: Its Measurement and Control in Science and Industry*, vol. 7, ed. by D.C. Ripple (AIP, Melville, New York, 2003), pp. 657–662
3. M. Battuello, F. Girard, T. Ricolfi, M. Sadli, P. Ridoux, O. Enouf, J. Pérez, V. Chimenti, T. Weckström, O. Struss, E. Filipe, N. Machado, E. van der Ham, G. Machin, H. McEvoy, B. Gutschwager, J. Fischer, V. Schmidt, S. Clausen, J. Ivarsson, S. Ugur, A. Diril, in *Temperature: Its Measurement and Control in Science and Industry*, vol. 7, ed. by D.C. Ripple (AIP, Melville, New York, 2003), pp. 903–908
4. T. Ricolfi, F. Girard, in *Proceedings of TEMPMEKO '99, 7th International Symposium on Temperature and Thermal Measurements in Industry and Science*, ed. by J.F. Dubbeldam, M.J. de Groot (Edauw Johannissen bv, Delft, 1999), pp. 593–598
5. H.C. McEvoy, G. Machin, N.P. Fox, E. Theocharous, I.S. Hassan, in *Proceedings of TEMPMEKO '96, 6th International Symposium on Temperature and Thermal Measurements in Industry and Science*, ed. by P. Marcarino (Levrotto and Bella, Torino, 1997), pp. 245–250
6. J. Fischer, B. Gutschwager, in *Proceedings of TEMPMEKO '96, 6th International Symposium on Temperature and Thermal Measurements in Industry and Science*, ed. by P. Marcarino (Levrotto and Bella, Torino, 1997), pp. 251–256
7. J. Fischer, in *Proceedings of TEMPMEKO '99, 7th International Symposium on Temperature and Thermal Measurements in Industry and Science*, ed. by J.F. Dubbeldam, M.J. de Groot (Edauw Johannissen bv, Delft, 1999), pp. 27–34
8. B. Gutschwager, J. Fischer, in *Proceedings of TEMPMEKO '99, 7th International Symposium on Temperature and Thermal Measurements in Industry and Science*, ed. by J.F. Dubbeldam, M.J. de Groot (Edauw Johannissen bv, Delft, 1999), pp. 567–572
9. F. Sakuma, J. Ishii, M. Kobayashi, in *TEMPBEIJING'97* (Standard Press of China, 1997), pp. 78–83
10. F. Sakuma, L. Ma, T. Kobayashi, in *Proceedings of TEMPMEKO 2007*, Int. J. Thermophys. **29**, 312 (2008), doi:10.1007/s10765-007-0340-6
11. Y. Shimizu, J. Ishii, F. Sakuma, A. Ono, in *Proceedings of TEMPMEKO 2004, 9th International Symposium on Temperature and Thermal Measurements in Industry and Science*, ed. by D. Zvizdić, L.G. Bermanec, T. Veliki, T. Stašić (FSB/LPM, Zagreb, Croatia, 2004), pp. 509–514
12. F. Sakuma, S. Hattori, in *Temperature: Its Measurement and Control in Science and Industry*, vol. 5, ed. by J.F. Schooley (AIP, New York, 1982), pp. 421–427
13. P. Saunders, D.R. White, Metrologia **41**, 41 (2004)
14. J. Ishii, M. Kobayashi, F. Sakuma, Metrologia **35**, 175 (1998)
15. J. Ishii, A. Ono, Meas. Sci. Technol. **12**, 2103 (2001)
16. J. Fischer, P. Saunders, M. Sadli, M. Battuello, C.W. Park, Y. Zundong, H. Yoon, W. Li, E. van der Ham, F. Sakuma, Y. Yamada, M. Ballico, G. Machin, N. Fox, J. Hollandt, M. Matveyev, P. Bloembergen, S. Ugur, CCT working document (in preparation)
17. Science Dictionary, 5th edn. (Iwanami Pub. Comp., Tokyo, 1998), p. 328 [in Japanese]
18. P. Saunders, J. Fischer, M. Sadli, M. Battuello, C.W. Park, Z. Yuan, H. Yoon, W. Li, E. van der Ham, F. Sakuma, J. Ishii, M. Ballico, G. Machin, N. Fox, J. Hollandt, M. Matveyev, P. Bloembergen, S. Ugur, in *Proceedings of TEMPMEKO 2007*, Int. J. Thermophys., doi: 10.1007/s10765-008-0385-1